Supporting Information

Sacrificial template synthesis of hollow-structured NiCoP microcubes as novel electrode material for asymmetric supercapacitors

Xiaobo Chen *, Yefei Zhuang

School of Physics and Electronic Engineering, Jiangsu Intelligent Optoelectronic Device and Measurement and Control Engineering Research Center, Yancheng Teachers University, Yancheng, 224051, PR China

* Correspondence: chenxbok@126.com

Experimental details

Structural characterizations

The X-ray diffraction (XRD) patterns recorded using a SHIMADZU XRD-6100 instrument with Cu-Kα radiation. The X-ray photoelectron spectra (XPS) were collected by a Thermo ESCALAB 250 electron spectrometer with an X-ray source of Al Ka. The scanning electron microscopy (SEM) imaging was conducted by Zeiss Supra 35VP scanning electron microscope, and the transmission electron microscopy (TEM) and high-resolution TEM (HRTEM) imaging was conducted by JEOL-2010 transmission electron microscope with 200 kV accelerated voltage.

Electrochemical measurements

All electrochemical tests were carried out on a CHI660E electrochemical workstation with the Ni foam carrying active material as the working electrode, Pt wire as the counter electrode was, and AgCl/Ag as the reference electrode. Besides, the electrolysis was 3 M KOH aqueous solution (50 mL). The galvanostatic charge/discharge (GCD) test and cycling test were conducted using a LAND battery program-control test system (CT2001A).

All working electrodes were fabricated by mixing the active material, carbon black, and polyvinylidene fluoride with a mass ratio of 85:10:5 in the N-methyl

pyrrolidone (NMP) solvent. Subsequently, the mixture was coated onto nickel foam and dried in a vacuum oven at 60 ◦C for 2 h. The mass loading of the active material on Ni foam is about 5.5 mg cm^{-2}.

The specific capacity C_s (C g^{-1}) of NiCo hydroxide and NiCoP electrodes is obtained from Equation (S1) [1].

$$C_s = I\Delta t/m \quad \text{(S1)}$$

where Δt (s) is the discharge time, I (A) is the applied current, m (g) is the is the loading mass of active material.

To explore the reaction kinetics, we further analyzed the linear correlation of the peak current (i) and sweep rate (v) based on the following formula [2]:

$$i = a \times v^b \quad \text{(S2)}$$

where (a, b) are constants, and the log (v) slope versus log(i) indicates the b-value which provides fundamental data about the charge storage kinetics.

The contribution ratio of capacitive and diffusion to the total charge storage can be determined from the CV curves using to the following equation, in which, $k_1 v$ stands for the capacitive controlled current and $k_1 v^{1/2}$ represents diffusion control process [3]:

$$i(\mathrm{V}) = k_1 v + k_2 v^{1/2} \quad \text{(S3)}$$

Fabrication of asymmetric supercapacitor device

In a two electrode system, the asymmetric supercapacitor (ASC) device was constructed by using the NiCoP hollow nanocubes as the positive electrode and AC as the negative electrode with a cellulose paper as the separator in 3 M KOH as electrolyte. Besides the capacity, charge balance between the cathode and anode also determines the ASC performance. To realize the charge balance, the active mass ratio of the cathode to anode was carefully decided according to the equation of $m_+/m_- = (C_- \Delta V_-)/(C_+ \Delta V_+)$, where m_+ and m_- are the active masses, C_+ and C_- are the specific capacities obtained by the three-electrode test, and ΔV_+ and ΔV_- are the potential windows of the cathode and anode, respectively. Based on the charge balance equation, the optimal mass loading of AC was estimated about 10.0 mg cm^{-2}.

The specific capacity C_{device} (C g^{-1}), specific energy E (Wh kg^{-1}) and specific power P (W kg^{-1}) of asymmetric supercapacitors can be calculated from the Equation (S2-S4), respectively [4, 5].

$$C_{device} = I\Delta t/m \quad \text{(S4)}$$

$$E = \frac{\int_{t1}^{t2} IV_{(t)}dt}{m \times 3.6} \quad \text{(S5)}$$

$$P = 3600E/\Delta t \quad \text{(S6)}$$

where I (A) corresponds to the applied current, Δt (s) means the discharging time, m (g) represents the total loading mass of active materials on both cathode and anode, t_1 (s) is the initial time after IR drop, t_2 (s) is the final time of discharge, and $\int V(t)\mathrm{d}t$ is the integrated area of discharge curves after IR drop.

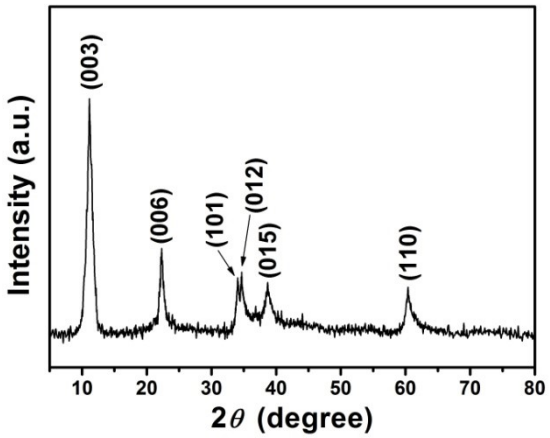

Fig. S1. X-ray diffraction pattern of NiCo hydroxide.

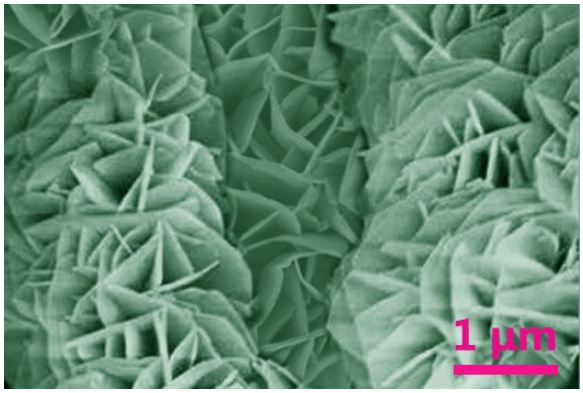

Fig. S2. SEM image of NiCoP-NSs.

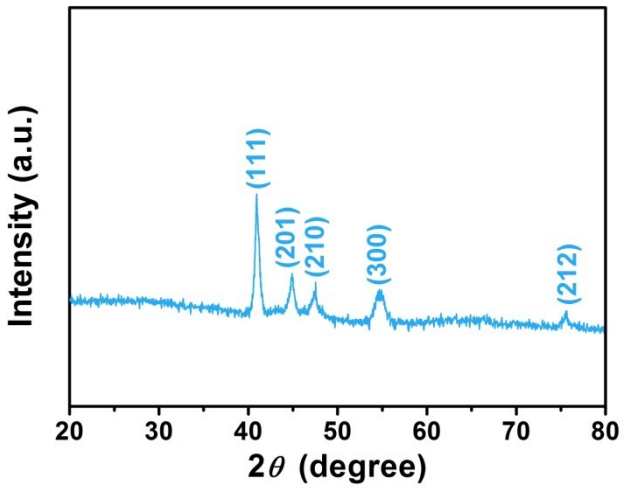

Fig. S3. X-ray diffraction pattern of NiCoP-NSs.

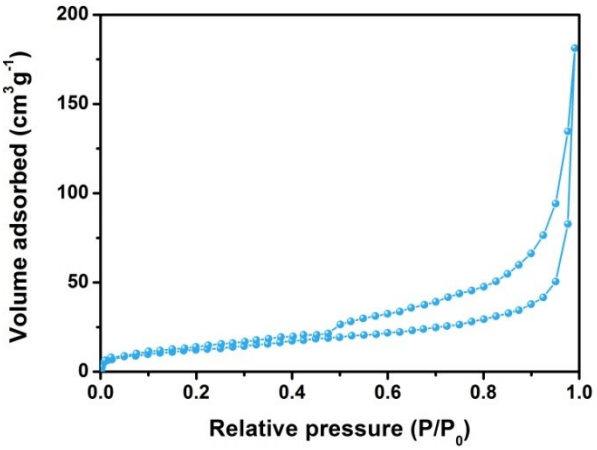

Fig. S4. Nitrogen adsorption/desorption isotherms of NiCoP-NSs.

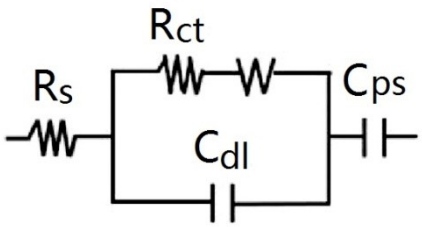

Fig. S5. The equivalent circuit diagram.

Table S1. Comparison of electrochemical performance with other electrodes reported in literatures.

Materials	Specific capacitance ($C\ g^{-1}$)	Capacitance retention (%)	Cycling stability (%) (current, cycles)	Ref.
NiCoP@NiCoP@CC	1125 C g^{-1} at 1 A g^{-1}	78.0% at 10 A g^{-1}	71.8% after 2000 cycles at 10 A g^{-1}	[6]
NiCoP/C	775.7C g^{-1} at 1 A g^{-1}	75.1% at 20 A g^{-1}	\	[7]
$NiCo_2S_4$/MXene	1028 C g^{-1} at 1 A g^{-1}	80.73 at 10 A g^{-1}	94.27% after 5000 cycles at 5 A g^{-1}	[8]
NiCoP@$MoSe_2$	5613.5 mF cm^{-2} (2245.4 F g^{-1}) at 1 mA cm^{-2}	79.2% at 40mA cm^{-2}	91.9% after 8000 cycles at 20 mA cm^{-2}	[9]
FeCoP@NiCoP/CC	973.0 C g^{-1} at 1 A g^{-1}	84.3% at 20A g^{-1}	84.7% after 5000 cycles at 5 A g^{-1}	[10]
$NiCo_2S_4$@NiCoP/NF	5.98 F/cm2 at 1 mA/cm^2	70.29% at 50 mA/cm^2	92.94% after 5000 cycles at 10 mA/cm^2	[11]
NiCoP nanorods	273.4 μAh cm^{-2} at 1 mA cm^{-2}	85.6% at 30 mA cm^{-2}	82.1% after 4000 cycles at 20 mA cm^{-2}	[12]
NiCoP microflowers	1153 F g^{-1} at 1 A g^{-1}	62% at 30 A g^{-1}	97% after7000 cycles at 20 A g^{-1}	[13]
CoP-Mn_3P nanoclusters	2714 F g^{-1} at 1 A g^{-1}	65.1% at 10 A g^{-1}	83.1% after 10,000 cycles	[14]
NiCoP/NC	1127 F g^{-1} at 1 A g^{-1}	77.5% at 16 A g^{-1}	75.5% after 8000 cycles at 40 mV s^{-1}	[15]
NiCoP nanocubes	1088.9 C g^{-1} at 1 A	88.7% at 10 A g^{-1}	90.2% after 10,000	This work

Materials	Specific capacitance ($C\ g^{-1}$)	Capacitance retention (%)	Cycling stability (%) (current, cycles)	Ref.
	g^{-1}		cycles at 1 A g^{-1}	

Table S2. A comparison on the specific capacitance, specific energy, specific power and cycle performance of NiCoP//AC ACS with the previously reported ASCs devices.

Electrode material	Specific capacity at current density	Specific energy ($Wh\ kg^{-1}$)	Specific power ($W\ kg^{-1}$)	Cycle Performance	Ref.
MnCoP//AC	237.74 C g^{-1} at 36 mA cm^{-2}	66.98	2550	94.7% after 6000 cycles at 36 mA cm^{-2}	[16]
NiCo-LDH/10//CNT	153.8 F g^{-1} at 1 A g^{-1}	36.1	649	103.9% after 5000 cycles at 4 A g^{-1}	[17]
CC/NiCoP@NiCo-LDH//AC	142 F g^{-1} at 1 A g^{-1}	57	850	97% after 10000 cycles at 5 A g^{-1}	[18]
FeCoP@NiCoP//BPC-800	206.3 F g^{-1} at 1 A g^{-1}	75.9	827.8	89.7% after 10000 at 7 A g^{-1}	[10]
$NiCo_2S_4$@NiCoP/NF//AC	429 mF/cm^2 at 1 mA/cm^2	0.135 mWh/cm^2	0.755 mW/cm^2	\	[19]
NiCoP//AC	264.6 μAh cm^{-2} at 2 mA cm^{-2}	85	644.3	86.3% after 8000 cycles at 20 mA cm^{-2}	[12]

Electrode material	Specific capacity at current density	Specific energy (Wh kg^{-1})	Specific power (W kg^{-1})	Cycle Performance	Ref.
CoP-Mn_3P//AC	130.4 F g^{-1} at 1A g^{-1}	46.4	800.0	86.2% after 30,000 cycles	[14]
NiCoP/NC//AC	167 F g^{-1} at 1 A g^{-1}	52	750	83.2% after 5000 cycles at 40 mV s^{-1}	[15]
NiCoP//AC	220.1 F g^{-1} at 1 A g^{-1}	78.2	799.9	84.8% after 10000 cycles at 8 A g^{-1}	This work

References

[1] G. Wei, X. Zhao, K. Du, Y. Huang, C. An, S. Qiu, M. Liu, S. Yao, Y. Wu, Flexible asymmetric supercapacitors made of 3D porous hierarchical $CuCo_2O_4$@CQDs and Fe_2O_3@CQDs with enhancedperformance. Electrochim. Acta 283 (2018) 248-259.

[2] W. Lu, J. Shen, P. Zhang, Y. Zhong, Y. Hu, X. W. Lou, Construction of CoO/Co-Cu-S hierarchical tubular heterostructures for hybrid supercapacitors. Angewandte Chemie, 131 (2019) 15587-15593.

[3] K. A. Sree Raj, A. S. Shajahan, B. Chakraborty, C. S. Rout, Two‐Dimensional Layered Metallic VSe_2/SWCNTs/rGO Based Ternary Hybrid Materials for High Performance Energy Storage Applications. Chem.-Eur. J. 26 (2020) 6662-6669.

[4] P. Bandyopadhyay, X. Li, N. H. Kim, J. H. Lee, Graphitic carbon nitride modified graphene/NiAl layered double hydroxide and 3D functionalized graphene for solid-state asymmetric supercapacitors, Chem. Eng. J. 353 (2018) 824-838.

[5] M. M. Vadiyar, X. Liu, Z. Ye, Highly porous silver dendrites on carbon nanotube wrapped copper cobaltite nano-flowers for boosting energy density and cycle stability of asymmetric supercapattery, J. Power Sources 415 (2019) 154-164.

[6] Y. Zhu, Q. Zong, Q. Zhang, H. Yang, Q. Wang, H. Wang, Three-dimensional core-shell NiCoP@NiCoP array on carbon cloth for high performance flexible asymmetric supercapacitor. Electrochim. Acta 299 (2019) 441-450.

[7] Q. Zhou, Y. Gong, K. Tao, Calcination/phosphorization of dual Ni/Co-MOF into NiCoP/C nanohybrid with enhanced electrochemical property for high energy density asymmetric supercapacitor. Electrochim. Acta 320 (2019) 134582.

[8] J. Fu, L. Li, J. M. Yun, D. Lee, B. K. Ryu, K. H. Kim, Two-dimensional titanium carbide (MXene)-wrapped sisal-Like $NiCo_2S_4$ as positive electrode for High-performance hybrid pouch-type asymmetric supercapacitor. Chem. Eng. J. 375 (2019) 121939.

[9] X. Gao, L. Yin, L. Zhang, Y. Zhao, B. Zhang, Decoration of NiCoP nanowires with interlayer-expanded few-layer $MoSe_2$ nanosheets: a novel electrode material for asymmetric supercapacitors. Chem. Eng. J. 395 (2020) 125058.

[10] L. Wan, Y. Wang, Y. Zhang, C. Du, J. Chen, M. Xie, Z. Tian, W. Zhang, Designing FeCoP@NiCoP heterostructured nanosheets with superior electrochemical performance for hybrid supercapacitors. J. Power Sources 506 (2021) 230096.

[11] X. Chang, W. Li, Y. Liu, M. He, X. Zheng, J. Bai, Z. Ren, Hierarchical $NiCo_2S_4$@NiCoP core-shell nanocolumn arrays on nickel foam as a binder-free supercapacitor electrode with enhanced electrochemical performance. J. Colloid Interf. Sci. 538 (2019) 34-44.

[12] Z. Wang, H. Wang, S. Ji, X. Wang, P. Zhou, S. Huo, V. Linkov, R. Wang, Hollow-structured NiCoP nanorods as high-performance electrodes for asymmetric supercapacitors. Mater. Design 193 (2020) 108807.

[13] Y. Jin, C. Zhao, Q. Jiang, C. Ji, Mesoporous NiCoP microflowers as a superior electrode material for supercapacitors. Appl. Surf. Sci. 450 (2018) 170-179.

[14] F. Xiang, Y. Dong, X. Yue, Q. Zheng, D. Lin, High-capacity CoP-Mn_3P nanoclusters heterostructures derived by Co_2MnO_4 as advanced electrodes for supercapacitors. J. Colloid Interf. Sci. 611 (2022) 654-661.

[15] T. Zhao, C. Liu, F. Yi, X. Liu, A. Gao, D. Shu, J. Ling, Promoting high-energy supercapacitor performance over NiCoP/N-doped carbon hybrid hollow nanocages via rational architectural and electronic modulation. Appl. Surf. Sci. 569 (2021) 151098.

[16] M. Amiri, S. E. Moosavifard, S. S. H. Davarani, S. K. Kaverlavani, M. Shamsipur, MnCoP hollow nanocubes as novel electrode material for asymmetric supercapacitors. Chem. Eng. J. 420 (2021) 129910.

[17] R. Ramachandran, Y. Lan, Z. X. Xu, F. Wang, Construction of NiCo-layered double hydroxide microspheres from Ni-MOFs for high-performance asymmetric supercapacitors. ACS Appl. Energy Mater. 3 (2020) 6633-6643.

[18] X. Gao, Y. Zhao, K. Dai, J. Wang, B. Zhang, X. Shen, NiCoP nanowire@NiCo-layered double hydroxides nanosheet heterostructure for flexible asymmetric supercapacitors. Chem. Eng. J. 384 (2020) 123373.

[19] X. Chang, W. Li, Y. Liu, M. He, X. Zheng, J. Bai, Z. Ren, Hierarchical $NiCo_2S_4$@NiCoP core-shell nanocolumn arrays on nickel foam as a binder-free supercapacitor electrode with enhanced electrochemical performance. J. Colloid Interf. Sci. 538 (2019) 34-44.